Available online at www.sciencedirect.com
SCIENCE DIRECT®
Thermochimica Acta 403 (2003) 237–249
thermochimica acta
www.elsevier.com/locate/tca

Thermal decomposition of the vivianite arsenates—implications for soil remediation

Ray L. Frost*, Matt L. Weier, Wayde Martens, J. Theo Kloprogge, Zhe Ding

Centre for Instrumental and Developmental Chemistry, Queensland University of Technology, GPO Box 2434, Brisbane, Qld 4001, Australia

Received 15 August 2002; accepted 5 January 2003

Abstract

The presence of arsenate compounds in soils and mineral dump leachates is common. One potential method for the removal of the arsenates from soils is through thermal treatment. High-resolution thermogravimetric analysis has been used to follow this thermal decomposition of selected vivianite arsenates. This decomposition occurs as a series of steps. The first two steps involve dehydration with 6 mol of water lost in the first step and two in the second. The third major weight loss step occurs in the 750–800 °C temperature range with de-arsenation. The application of infrared emission spectroscopy confirms the loss of water by around 250 °C and the loss of arsenic as arsenic pentoxide is observed by the loss of AsO stretching bands at around 826 cm^{-1}. Thermal activation of arsenic contaminated soils may provide a method of decontamination.

Keywords: Vivianite; Iron; Phosphate; Thermal analysis; Infrared emission spectroscopy

1. Introduction

Soils have been contaminated very heavily with arsenic compounds for a number of reasons [1–3]. Among the reasons for this soil contamination is the over use of arsenic based pesticides [1], from leaching of old mine sites [3,4], pollution from the use of Cu/Cr/As wood preservatives [5], from tannery wastes [6] and even from old munition sites [7]. These arsenic compounds may leach and infiltrate ground waters [8,9]. Soil remediation of the contaminated soils is an important environmental innovation and various methods may be employed. Heavy metal tolerant plants may be used; agglomeration techniques can be employed in which heavy metals are extracted [10]; soils may be leached with solutions for example of EDTA [11,12]; various chemicals may be added to the soil to complex with the arsenic compounds [13–15]; biological extraction of the arsenic is useful in innovative remediation [16–19]; the use of heavy metal tolerant plants may be useful at least as a starting step [20]. One other method that may be employed is through thermal decomposition since most arsenic compounds are volatile as the arsenic can be removed through its evolved gases.

Arsenic in soils may be reactive and various compounds may be formed. Among these compounds are the vivianite arsenates. These may be the compositionally related arsenate minerals such as parasymplesite, hornesite, kottigite and even annabergite and erythrite. These minerals have a formula $(M^{2+})_3(AsO_4)_2{\cdot}8H_2O$ where M is Ni, Co, Zn, Mg,

* Corresponding author. Tel.: +61-7-3864-2407; fax: +61-7-3864-1804.
E-mail address: r.frost@qut.edu.au (R.L. Frost).

0040-6031/03/$ – see front matter
doi:10.1016/S0040-6031(03)00046-7

or a cationic combination. It is likely that a complex set of solid solutions may be present in relation to the soil composition and the availability of the metals for chemical reaction. There have been some reports on the thermal analysis of these types of compounds [21–25]. Thermal decomposition studies show that the dissociation is complex [21]. The question of thermal treatment of arsenic compounds arises when CCA treated wood is combusted [26]. Few reports on the thermal decomposition of arsenates have been forthcoming and as an exemplary study in this paper we report the thermal decomposition of selected vivianite arsenates.

2. Experimental

2.1. Natural and synthetic vivianite

The natural vivianite arsenate minerals were obtained from BK minerals suppliers (Brisbane, Australia). Synthetic vivianite arsenates of Zn, Fe, Co and Ni were prepared by the slow addition of the 3.5×10^{-3} M metal sulphate solution to a very dilute 5.0×10^{-3} M sodium arsenate solution using a peristaltic pump at 70 °C. The hydrated cationic arsenates precipitated from the solution and were filtered and dried. The crystals were hydrothermally treated and were grown by Ostwald ripening at 70 °C for 14 days. Samples were analysed for phase purity by X-ray diffraction and for chemical composition by ICP-AES and also by electron probe analyses.

2.2. X-ray diffraction

The normal room temperature and temperature controlled XRD analyses were carried out on a Philips wide angle PW 3020/1820 vertical goniometer equipped with curved graphite-diffracted beam monochromators. The d-spacing and intensity measurements were improved by application of a self developed computer aided divergence slit system enabling constant sampling area irradiation (20 mm long) at any angle of incidence. The goniometer radius was enlarged from 173 to 204 mm. The radiation applied was Cu Kα from a long fine focus Cu tube, operating at 40 kV and 40 mA. The samples were measured in static air and in flowing nitrogen atmosphere at 15 l/h

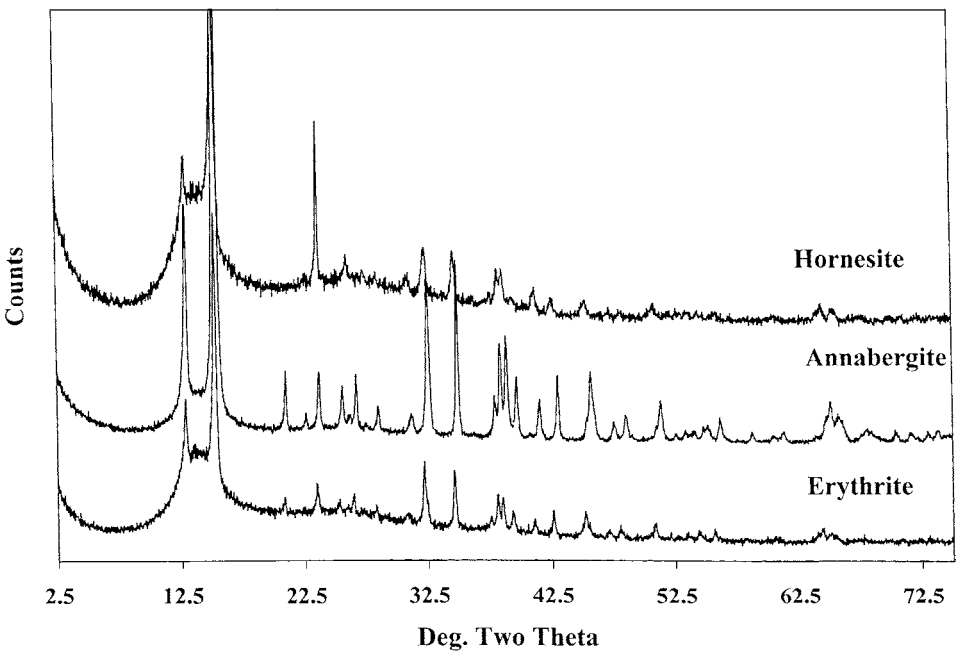

Fig. 1. X-ray diffraction patterns of erythrite, annabergite and hornesite.

in stepscan mode with steps of 0.025° 2θ and a counting time of 1 s. Measured data were corrected with the Lorentz polarisation factor (for oriented specimens) and for their irradiated volume.

2.3. Thermal analysis

Thermal decomposition of the arsenate was carried out in a TA® Instruments incorporated high-resolution

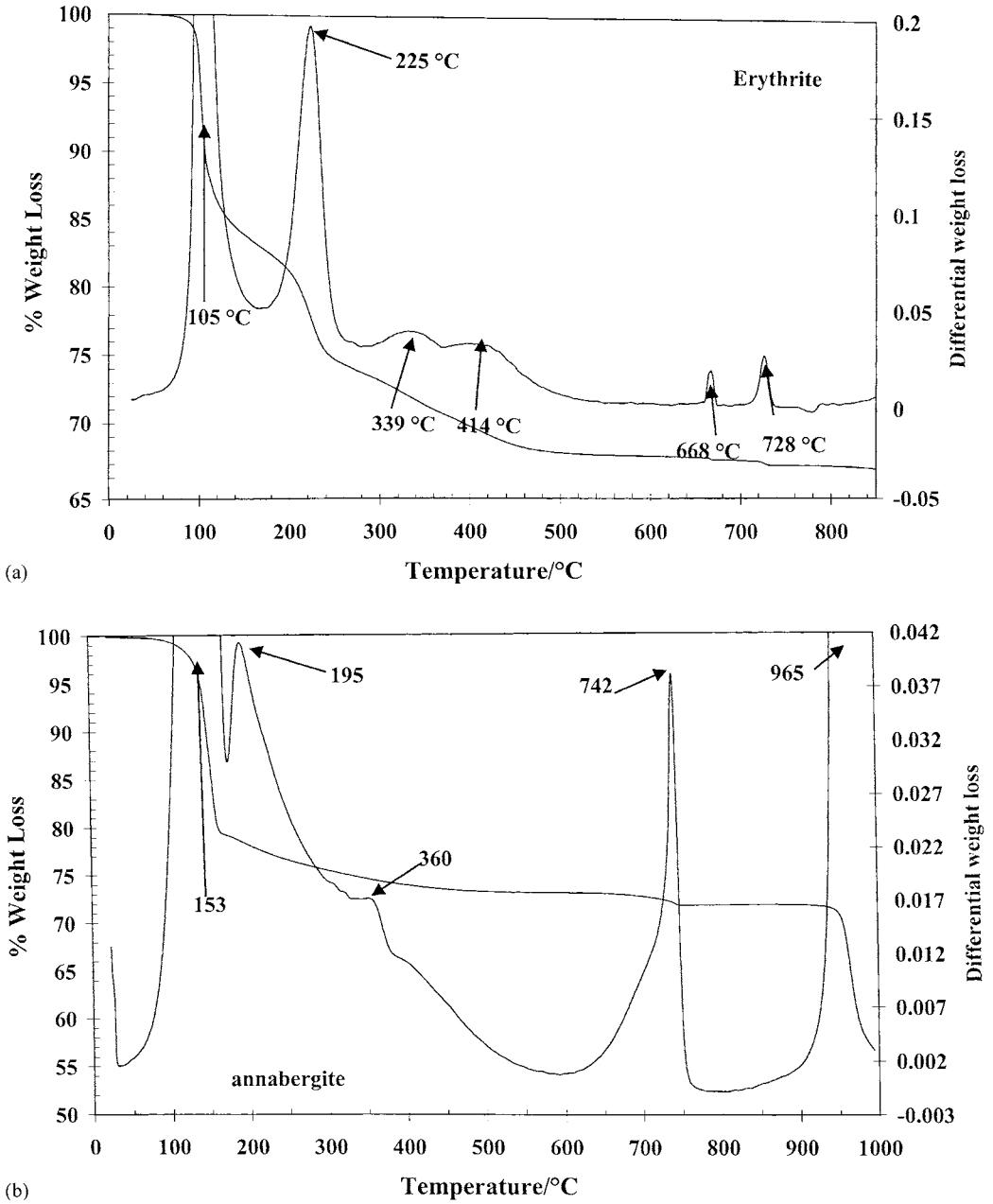

Fig. 2. (a) High resolution thermogravimetric analysis of erythrite; (b) annabergite; (c) hornesite; and (d) erythrite at elevated temperatures.

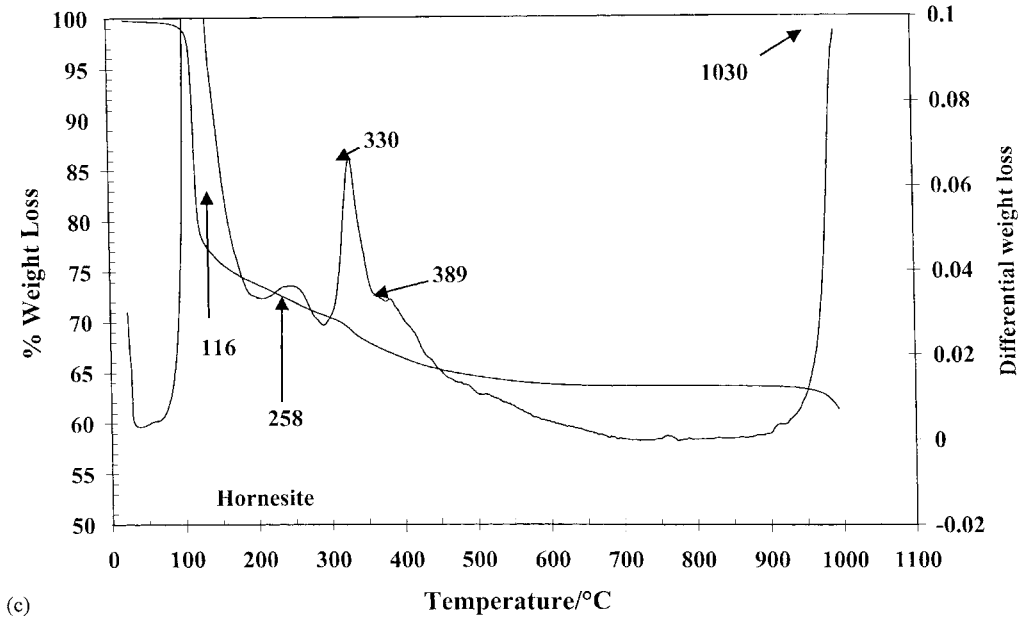

(c)

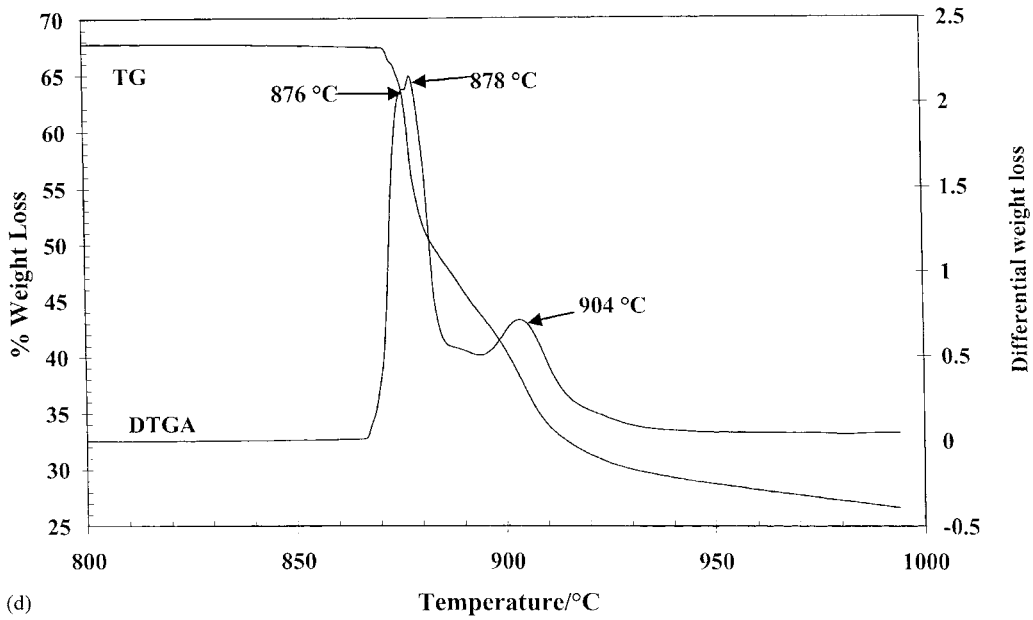

(d)

Fig. 2. (*Continued*).

thermogravimetric analyzer (series Q500) in a flowing nitrogen atmosphere (80 cm^3/min). Approximately 5 mg of sample was heated in an open platinum crucible at a rate of 2.0 °C/min up to 500 °C. With the quasi-isothermal, quasi-isobaric heating program of the instrument the furnace temperature was regulated precisely to provide a uniform rate of decomposition in the main decomposition stage. The TGA instrument

was coupled to a Balzers (Pfeiffer) mass spectrometer for gas analysis. Only selected gases were analyzed.

2.4. Infrared emission spectroscopy

FTIR emission spectroscopy was carried out on a Nicolet spectrometer equipped with a TGS detector, which was modified by replacing the IR source with an emission cell. A description of the cell and principles of the emission experiment have been published elsewhere [27–34]. Approximately 0.2 mg of vivianite mineral was spread as a thin layer (approximately 0.2 μ) on a 6 mm diameter platinum surface and held in an inert atmosphere within a nitrogen-purged cell during heating.

In the normal course of events, three sets of spectra are obtained: firstly the black body radiation over the temperature range selected at the various temperatures, secondly the platinum plate radiation is obtained at the same temperatures and thirdly the spectra from the platinum plate covered with the sample. Normally only one set of black body and platinum radiation is

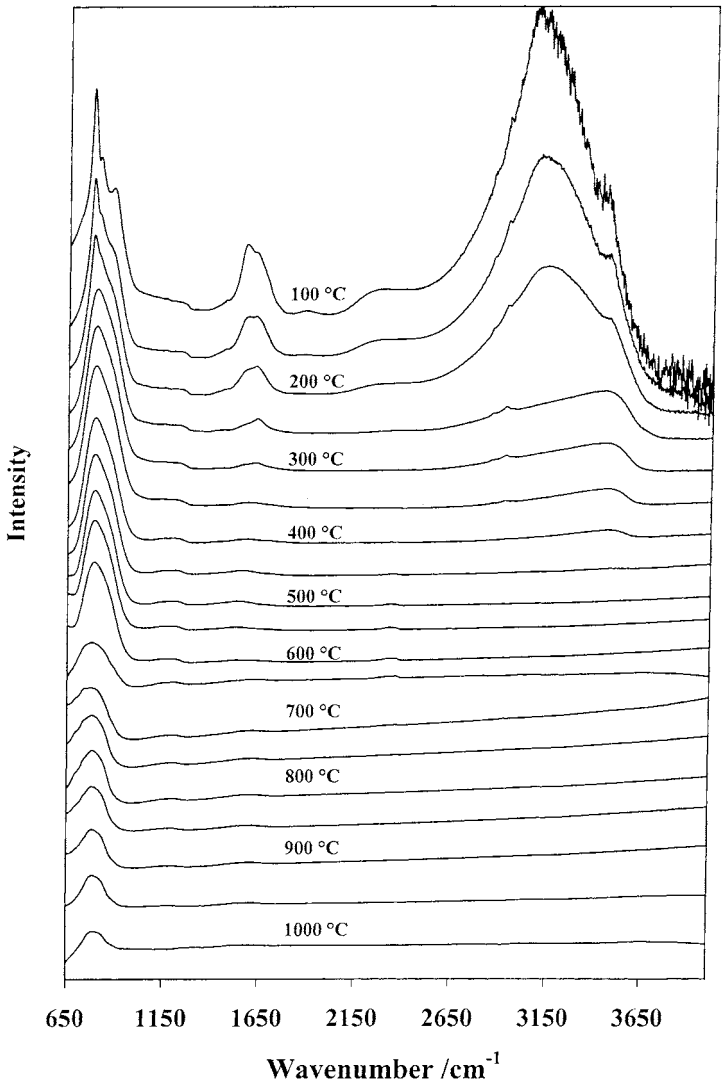

Fig. 3. Infrared emission spectra of erythrite.

required. The emittance spectrum (E) at a particular temperature was calculated by subtraction of the single beam spectrum of the platinum backplate from that of the platinum + sample, and the result ratioed to the single beam spectrum of an approximate blackbody (graphite). The following equation was used to calculate the emission spectra.

$$E = -0.5 \times \log \frac{\mathrm{Pt} - \mathrm{S}}{\mathrm{Pt} - \mathrm{C}}$$

This spectral manipulation is carried out after all the spectral data has been collected. The emission spectra were collected at intervals of 50 °C over the range 200–750 °C. The time between scans (while the temperature was raised to the next hold point) was approximately 100 s. It was considered that this was sufficient time for the heating block and the powdered sample to reach temperature equilibrium. The spectra were acquired by coaddition of 64 scans for the whole temperature range (approximate scanning

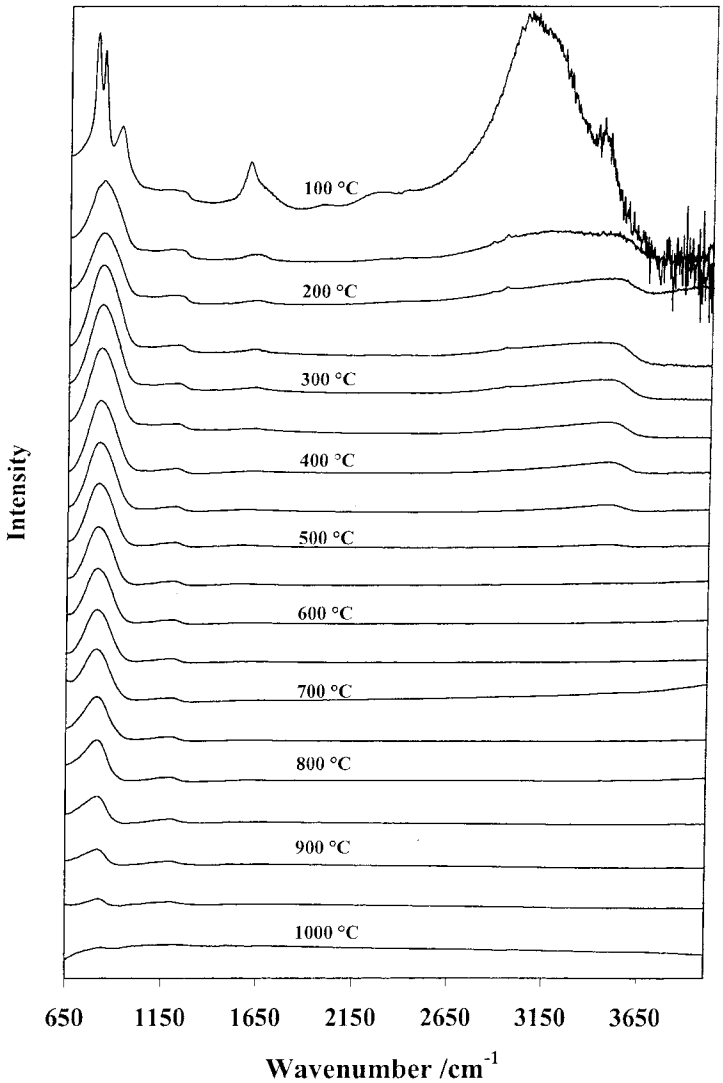

Fig. 4. Infrared emission spectra of annabergite.

time 45 s), with a nominal resolution of 4 cm^{-1}. Good quality spectra can be obtained providing the sample thickness is not too large. If too large a sample is used then the spectra become difficult to interpret because of the presence of combination and overtone bands. Spectral manipulation such as baseline adjustment, smoothing and normalisation was performed using the GRAMS® software package (Galactic Industries Corporation, Salem, NH, USA).

3. Results and discussion

3.1. X-ray diffraction

The X-ray diffraction patterns of the synthetic vivianite arsenates used in this research are shown in Fig. 1. The patterns correspond exactly with the database patterns and no impurities are observed. The X-ray diffraction patterns also show that annabergite is more crystalline than either erythrite or hornesite.

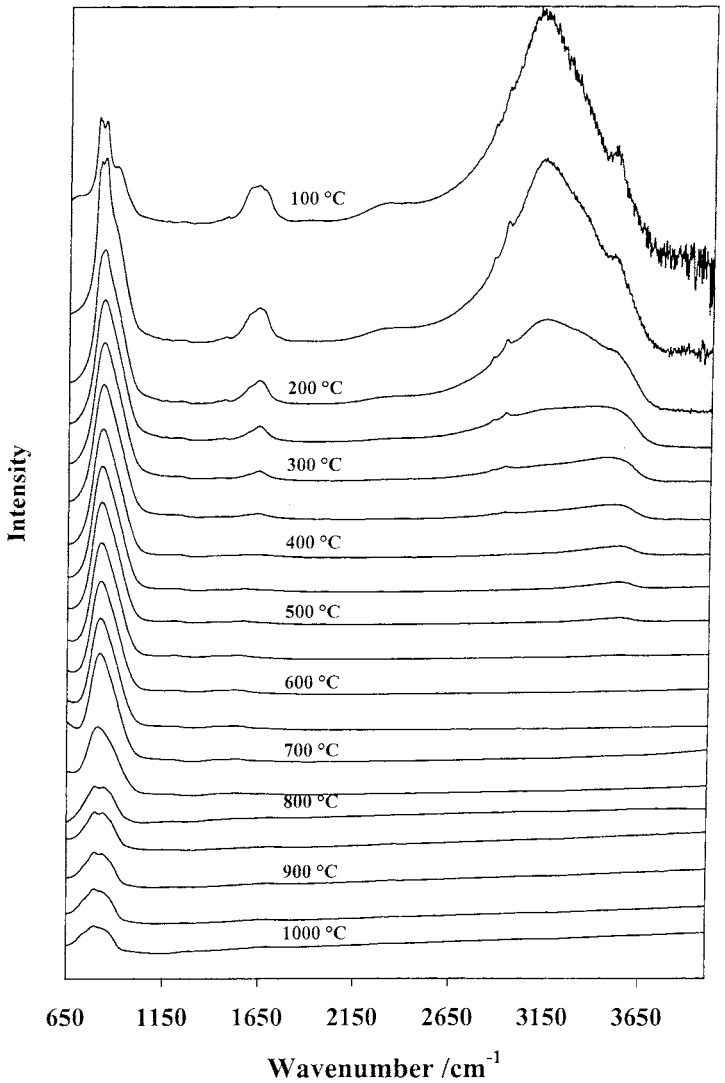

Fig. 5. Infrared emission spectra of hornesite.

3.2. Thermogravimetric analysis

The high resolution thermogravimetric analyses of erythrite, annabergite and hornesite are shown in Fig. 2. For erythrite there is a 21% weight loss at 105 °C and a 9% weight loss at 225 °C. Such weight losses suggest that 6 mol of water are lost in the first weight loss step and 2 mol in the second step. For

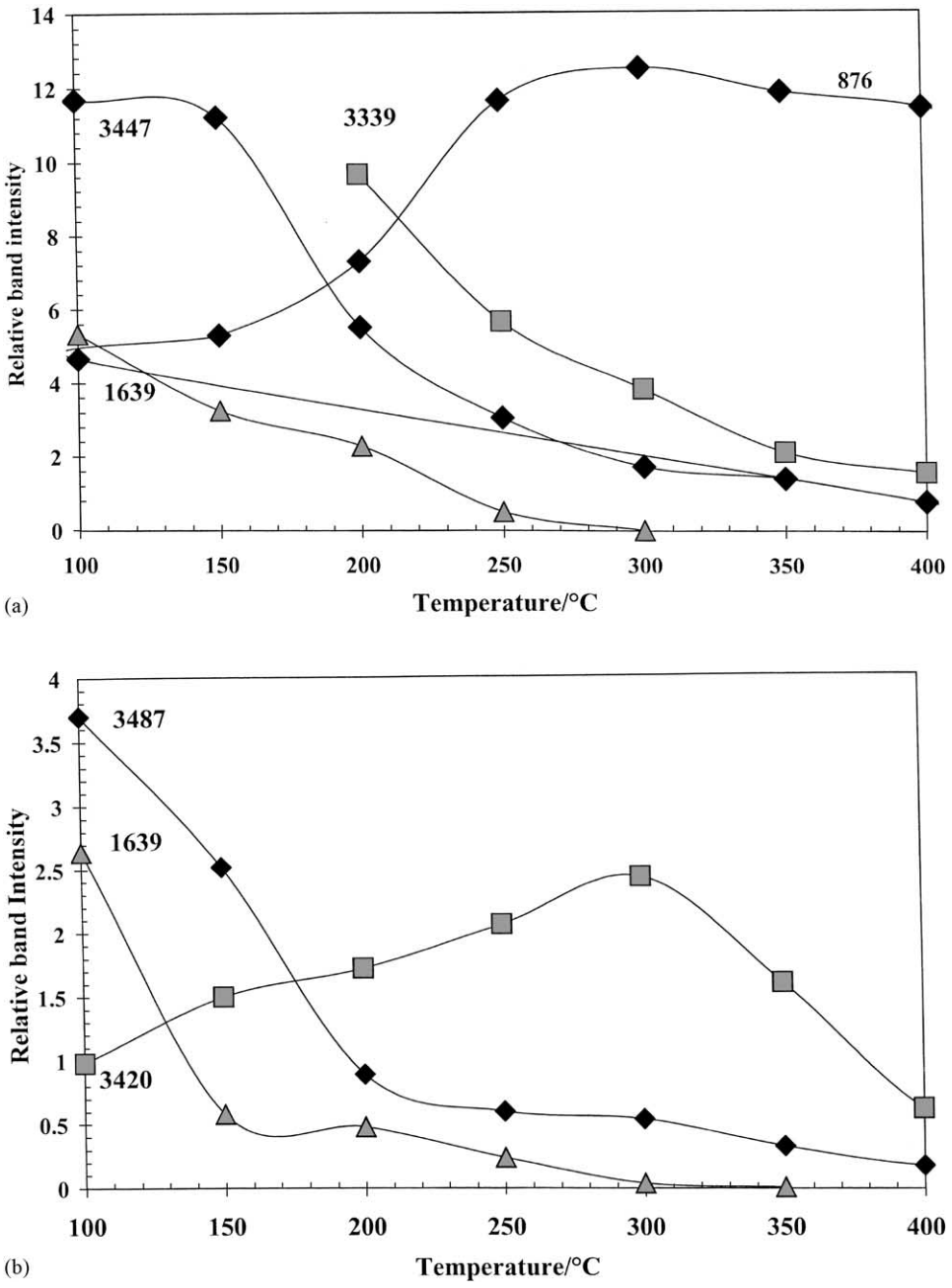

Fig. 6. (a) Variation of band intensity with temperature of erythrite (b) and annabergite.

Table 1
Results of the infrared emission spectroscopy of erythrite

	Temperature (°C)																		
	100	150	200	250	300	350	400	450	500	550	600	650	700	750	800	850	900	950	1000
Peak position	737	744	773											692	691	698	705		
Rel area	2.16	1.66	1.17											0.10	0.15	0.09	0.10		
Peak position	774	775	775	781	778	777	775	774	774	773	770	739	743	760	761	777	775	774	792
Rel area	3.54	7.40	0.41	13.23	12.76	12.77	10.83	9.89	3.99	3.28	2.94	1.20	2.20	3.81	4.41	4.00	2.77	3.02	4.67
Peak position	814	813	803									820	819	831	831	839	835	831	
Rel area	1.49	1.76	8.22									4.85	3.25	2.57	2.86	1.39	1.62	1.94	
Peak position	876	871	892	870	867	867	861	858	853	848	847	904							
Rel area	4.66	5.30	2.49	11.65	12.49	11.84	11.43	10.40	9.59	8.90	8.20	0.34							
Peak position	1177	1174		1167	1177	1171	1161	1159	1159	1155	1155	1147	1146	1144	1142	1139	1125	1107	948
Rel area	0.11	0.22		0.28	0.21	0.21	0.26	0.27	0.24	0.26	0.23	0.27	0.24	0.24	0.24	0.19	0.11	0.04	1.14
Peak position	1235	1237	1213	1232	1235	1232	1226	1223	1222	1219	1217	1211	1211	1208	1207	1205	1197	1182	1282
Rel area	0.11	0.19	0.36	0.19	0.15	0.17	0.20	0.19	0.16	0.16	0.15	0.12	0.12	0.10	0.10	0.10	0.10	0.08	0.09
Peak position	1565	1567	1570	1605	1616	1606	1590	1557	1542	1540	1562	1603	1575	1571	1563	1564	1566	1564	1564
Rel area	7.23	5.34	3.30	1.74	1.24	0.97	0.98	0.77	0.92	0.74	0.55	0.87	0.51	0.58	0.60	0.54	0.52	0.46	0.91
Peak position	1639	1639	1637	1638					2337	2331	2330	2317							
Rel area	5.33	3.25	2.28	0.51					0.09	0.10	0.11	0.09							
Peak position	2320	2280	2308	2355	2337	2336	2338					2365							
Rel area	13.04	5.84	3.94	0.54	0.15	0.01	0.02					0.04							
Peak position				2983	3001	3020													
Rel area				12.58	7.32	2.04													
Peak position	3113	3158	3153	3259	3271	3226	3109												
Rel area	176.49	112.68	45.91	8.56	5.95	2.25	0.90												
Peak position			3339	3417	3424	3367	3339												
Rel area			9.66	5.66	3.82	2.11	1.57												
Peak position	3447	3466	3483	3517	3513	3461	3456												
Rel area	11.68	11.21	5.51	3.05	1.73	1.40	0.79												

Table 2
Results of the infrared emission spectroscopy of annabergite

	Temperature (°C)																		
	100	150	200	250	300	350	400	450	500	550	600	650	700	750	800	850	900	950	1000
Peak position	741																		
Rel area	0.48																		
Peak position	788																		
Rel area	4.70																		
Peak position	826	830	830	829	809	805	793	794	787	789	782	778	761	727	766	758	764	766	
Rel area	2.85	8.59	4.18	5.85	4.25	3.80	2.83	2.87	2.20	4.25	2.06	1.44	0.44	0.16	1.59	0.53	0.34	0.09	
Peak position	912				891	885	870	871	861	862	847	847	825	814	828	828	829	828	833
Rel area	1.54				1.17	1.32	1.59	1.55	1.68	2.58	1.88	3.12	3.91	4.13	2.01	0.73	0.37	0.20	0.11
Peak position	1185	1179	1170	1132	1176	1172	1165	1165	1161	1157	1168	1151	1158	1152	1140	1157	1095	1092	
Rel area	0.36	0.49	0.52	0.26	0.24	0.21	0.20	0.20	0.23	0.26	0.20	0.26	0.22	0.25	0.32	0.44	0.22	0.18	
Peak position	1239	1236	1231	1220	1230	1227	1222	1222	1219	1216	1214	1211	1211	1209	1204	1207	1196	1195	1210
Rel area	0.15	0.16	0.17	0.31	0.14	0.13	0.12	0.13	0.13	0.12	0.10	0.12	0.10	0.11	0.14	0.09	0.35	0.46	0.08
Peak position	1626	1607	1613	1613	1610	1613	1564	1559	1579	1573		1632	1598	1622	1591	1599			
Rel area	2.64	0.58	0.48	0.61	0.51	0.39	0.27	0.22	0.36	0.25		0.40	0.19	0.26	0.20	0.23			
Peak position	1965				1629	1624	1734	1700											
Rel area	0.19				0.04	0.01	0.20	0.22											
Peak position	2231	2375	2330	2415													1631	1659	1686
Rel area	1.52	0.84	0.07	0.40													0.10	0.11	0.37
Peak position	3064	3141	2972	3017	3013														
Rel area	66.36	18.35	2.51	4.70	3.20														
Peak position			3248	3255	3241	3272	3198	3202											
Rel area			2.73	2.35	1.89	1.93	0.66	0.68											
Peak position	3426		3420	3414	3414	3430	3387	3387	3291										
Rel area	0.98		1.72	2.06	2.43	1.60	0.63	0.62	0.23										
Peak position		3487	3530	3524	3519	3515	3491	3491	3456										
Rel area		2.52	0.49	0.60	0.54	0.33	0.18	0.19	0.11										

Table 3
Results of the infrared emission spectroscopy of hornesite

	Temperature (°C)																		
	100	150	200	250	300	350	400	450	500	550	600	650	700	750	800	850	900	950	1000
Peak position	760														760	770	763	754	738
Rel area	6.13														25.70	35.42	32.41	38.54	9.27
Peak position	796	795	797																
Rel area	15.47	8.70	8.52																
Peak position	811	809		818	819	818	816	814	811	809	808	807	805	793	799	797	794	793	790
Rel area	2.56	1.77		50.12	54.39	58.37	58.85	56.81	51.53	49.13	47.57	43.82	41.20	34.62	20.47	6.09	5.42	9.36	26.86
Peak position	833	830	827																
Rel area	18.89	6.39	7.05																
Peak position			857												841	836	835	833	845
Rel area			70.14												2.77	5.75	29.49	13.63	35.46
Peak position	898	906		890	895	900	900	896	889	886	883	878	874	867	872	872	879	878	890
Rel area	21.50	16.91		40.76	39.74	37.34	37.55	39.86	45.09	48.17	49.71	52.60	54.65	59.11	42.92	44.24	26.36	33.72	8.28
Peak position							1213	1210	1209	1208	1213	1207	1199	1197	1192	1190	1194		1283
Rel area							0.41	0.42	0.43	0.45	0.34	0.38	0.39	0.49	0.87	0.90	0.65		2.92
Peak position	1454	1455	1450																
Rel area	2.00	1.31	0.96																
Peak position	1586	1593		1587				1580	1557	1532	1519	1514	1512	1524	1497	1511	1542	1560	1483
Rel area	19.68	9.97		4.20				2.92	2.95	2.25	2.38	3.21	3.76	5.78	3.72	2.40	2.22	1.90	6.48
Peak position	1629		1611	1645	1632	1626	1606												
Rel area	1.68		8.94	4.93	5.87	4.29	3.19												
Peak position	1666	1656	1651												1690	1686	1680	1666	1672
Rel area	12.08	7.29	4.38												3.54	5.19	3.45	2.85	10.74
Peak position				2944		2936													
Rel area				35.38		27.96													
Peak position	3120	3125	3142				3089	3064											
Rel area	82.94	48.53	40.40				24.13	0.30											
Peak position				3214	3197	3234		3244											
Rel area				31.53	29.14	31.62		23.02											
Peak position		3328	3373		3354		3313		3336										
Rel area		11.13	17.01		14.73		5.88		17.42										
Peak position				3423	3481	3437	3471	3431	3477										
Rel area				18.60	17.83	26.56	58.25	48.28	61.21										
Peak position	3491	3497	3527	3546	3569	3549	3548	3541	3551										
Rel area	4.90	11.34	9.39	8.89	6.93	12.75	11.51	28.40	21.37										

annabergite two weight loss steps are observed at 153 and 195 °C. The effect of crystallinity is the reason why the first dehydration step occurs at the higher temperature compared to that of erythrite. The dehydration steps for hornesite occur at 116 and 258 °C. It is suggested that the crystallinity and particle size of the minerals effects the dehydration temperatures.Thus, dehydration of these minerals occurs in two steps as follows:

$$(M^{2+})_3(AsO_4)_2 \cdot 8H_2O \rightarrow (M^{2+})_3(AsO_4)_2 \cdot 2H_2O + 6H_2O$$

$$(M^{2+})_3(AsO_4)_2 \cdot 2H_2O \rightarrow (M^{2+})_3(AsO_4)_2 + 2H_2O$$

where M = Co, Ni, Mg.

Minor weight loss steps occur for erythrite at 339, 414, 668 and 728 °C. A large weight loss step is observed for all three minerals in the 800–1100 °C temperature range. Fig. 3 shows the HRTGA plot for erythrite. Weight loss steps are observed at 877 and 904 °C. The weight loss is due to the loss of As_2O_5 units and chemical reactions are:

$$2(M^{2+})_3(AsO_4)_2 \rightarrow 2M^{2+}O + (M^{2+})_3(AsO_4)_2 + As_2O_5$$

$$(M^{2+})_3(AsO_4)_2 \rightarrow 2M^{2+}O + As_2O_5$$

The temperatures for the decomposition of annabergite and hornesite occur at slightly higher temperatures above the limits of the HRTGA instrument. Coupling of the HR-TGA with a mass spectrometer was attempted but blockage of the capillary between the TGA furnace and the MS occurred preventing useful MS measurements to be obtained.

3.3. Infrared emission spectroscopy

The infrared emission spectra as a function of temperature of erythrite, annabergite and hornesite are shown in Figs. 3–5, respectively. The spectroscopic analysis is tabulated in Tables 1–3 for the respective minerals. The spectra quite clearly show the loss in intensity of bands in the 3000–3700 cm^{-1} region attributed to the hydroxyl-stretching region. The spectra in this region for erythrite and hornesite appear similar but the spectrum of annabergite is different. The spectra may be divided into three sections: (a) hydroxyl-stretching region (b) water HOH bending region and (c) arsenate AsO stretching region. In the 100 °C spectrum of the hydroxyl-stretching region bands are resolved at 3451, 3284 and 3135 cm^{-1}. The band at around 3451 cm^{-1} is observed in the lower temperature spectra of all three vivianite arsenates. The band is attributed to an AsOH stretching vibration. The band is lost by 250 °C. The two bands at 3284 and 3135 cm^{-1} are attributed to the OH stretching bands of water.

Fig. 6 displays the decrease in intensity of selected bands as a function of temperature. The figure clearly demonstrates the loss of intensity of the hydroxyl-stretching bands of water as a function of time. Concomitantly the loss of intensity of the water HOH deformation mode is also observed. The loss of intensity demonstrates that dehydration of the mineral has occurred by around 250 °C for erythrite and by 200 °C for annabergite. Similar results are observed for hornesite. At the same time the intensity of the AsO stretching vibration increases in relative intensity. At around 250 °C the intensity is at a maximum and a significant decrease in intensity is observed in the 700–750 °C temperature range until at 750 °C the intensity approached zero. Thus, this is the temperature range where the loss of arsenic as As_2O_5 occurs. In a previous study the thermal analysis patterns obtained using DTA methods, an endothermic peak at around 730 °C was observed for erythrite, annabergite, koettigite and hornesite [35]. This author rightly pointed out that the vivianite arsenate minerals can be distinguished through their thermal analysis patterns and that significant differences are observed in the patterns between different mineral species of the group. Such observations are also observed in the decrease in intensity of the infrared emission bands of erythrite and annabergite.

4. Conclusions

The contamination of soils through arsenic poisoning has been occurring for an extensive period of time. In the case of cattle dips in Australia for much more than 100 years. One method of treatment of heavily contaminated soils may be through thermal treatment and volatilisation of the arsenic as As_2O_5. The de-arsenation of the soil through volatilisation

of the arsenic as As_2O_5 and its breakdown products creates a secondary problem in that the arsenic condensates will need to be collected and further disposed.

High resolution thermogravimetric analysis has been used to follow the thermal decomposition of a common group of arsenic minerals, namely the vivianite arsenates. Both dehydration and de-arsenation is mineral dependent and probably depends on a number of factors such as crystallinity and crystal size. Dehydration occurs in two steps in the 105–150 °C temperature range and the second step over the 150–250 °C temperature range. De-arsenation appears to occur at around 750 °C. Changes in the structure of the vivianite arsenates are readily followed by the use of infrared emission spectroscopy. Variation in the intensity of the water OH stretching and bending vibrations can be used to determine the temperatures for dehydration of the vivianite arsenates. The temperatures obtained using the IES technique support the results as determined by HR-TGA.

Acknowledgements

The financial and infra-structure support of the Queensland University of Technology Centre for Instrumental and Developmental Chemistry is gratefully acknowledged. The Australian research Council (ARC) is thanked for funding the purchase of the thermo-analytical facility.

References

[1] H. Akhter, F.K. Cartledge, J. Miller, M. Mclearn, J. Environ. Eng. (Reston, Virginia) 126 (2000) 999.
[2] P. Alumaa, U. Kirso, V. Petersell, E. Steinnes, Int. J. Hygiene Environ. Health 204 (2002) 375.
[3] E.H. Amonoo-Neizer, D. Nyamah, S.B. Bakiamoh, Water, Air, Soil Pollut. 91 (1996) 363.
[4] P.M. Ashley, B.G. Lottermoser, Australian J. Earth Sci. 46 (1999) 861.
[5] C.F. Balasoiu, G.J. Zagury, L. Deschenes, Sci. Total Environ. 280 (2001) 239.
[6] R. Sadler, H. Olszowy, G. Shaw, R. Biltoft, D. Connell, Water, Air, Soil Pollut. 78 (1994) 189.
[7] Beletskaya, Bilger, Boronin, Bunnett, Costantino, Cullen, Dominas, Goessler, Haiduc, Maeda and Martens, NATO ASI Series, Ser. 1 Disarmament Technol. 19 (1998) 177.
[8] D. Chakraborti, G. Samanta, B.K. Mandal, T.R. Chowdhury, C.R. Chanda, B.K. Biswas, R.K. Dhar, G.K. Basu, K.C. Saha, Curr. Sci. 74 (1998) 346.
[9] D.K. Bhumbla, R.F. Keefer, Adv. Environ. Sci. Technol. 26 (1994) 51.
[10] A. Majid, S. Argue, Min. Eng. 14 (2001) 1513.
[11] N. Papassiopi, S. Tambouris, A. Kontopoulos, Water, Air, Soil Pollut. 109 (1999) 1.
[12] T. Xie, W.D. Marshall, J. Environ. Monit. 3 (2001) 411.
[13] N. Yossapol, J.N. Meegoda, Hazard. Industrial Wastes 32nd (2000) 787.
[14] T.J. Moore, C.M. Rightmire, R.K. Vempati, Soil Sediment Contam. 9 (2000) 375.
[15] J.R. Davenport, F.J. Peryea, Water, Air, Soil Pollut. 57–58 (1991) 101.
[16] R.D. Bardgett, T.W. Speir, D.J. Ross, G.W. Yeates, H.A. Kettles, Biol. Fertil. Soils 18 (1994) 71.
[17] V. Dutre, C. Kestens, J. Schaep, C. Vandecasteele, Sci. Total Environ. 220 (1998) 185.
[18] R. Gourdon, N. Funtowicz, Soil Environ. 5 (1995) 1049.
[19] V.I. Groudeva, S.N. Groudev, A.S. Doycheva, Process Metal. 11B (2001) 443.
[20] E. Lombi, W.W. Wenzel, D.C. Adriano, Environ. Sci. Pollut. Control Series 23 (2000) 739.
[21] P.K. Gallagher, Thermochim. Acta 14 (1976) 131.
[22] A.Z. Beilina, K.M. Zhumanova, Z.M. Muldakhmetov, R.S. Khalimova, Zh. Fiz. Khim. 51 (1977) 480.
[23] L.S. Bark, A.E. Nya, J. Therm. Anal. 12 (1977) 277.
[24] M.I. Zhambekov, S.M. Isabaev, B.K. Kasenov, Zh. Fiz. Khim. 50 (1976) 1050.
[25] K.M. Zhumanova, A.Z. Beilina, Z.M. Muldakhmetov, Khim.-Metall. Inst., Karaganda, USSR. FIELD URL:, 1977, p. 13.
[26] A.K. Kercher, D.C. Nagle, Wood Sci. Technol. 35 (2001) 325.
[27] R.L. Frost, B.M. Collins, K. Finnie, A.J. Vassallo, in: Proceedings of the 10th International Clay Conference: Clay Controlling the Environment, Adelaide, Australia, 1995, p. 219.
[28] R.L. Frost, A.M. Vassallo, Clays Clay Miner. 44 (1996) 635.
[29] R.L. Frost, A.M. Vassallo, Mikrochim. Acta (Suppl. 14) (1997) 789.
[30] R.L. Frost, J.T. Kloprogge, S.C. Russel, J. Szetu, Appl. Spectrosc. 53 (1999) 829.
[31] R.L. Frost, J.T. Kloprogge, S.C. Russel, J. Szetu, Appl. Spectrosc. 53 (1999) 572.
[32] J.T. Kloprogge, R.L. Frost, Appl. Clay Sci. 15 (1999) 431.
[33] J.T. Kloprogge, R.L. Frost, J. Kristof, Can. J. Anal. Sci. Spectrosc. 44 (1999) 33.
[34] J.T. Kloprogge, R.L. Frost, Neues Jahrb. Miner., Montash (2000) 145.
[35] R. Pulou, Compt. rend. 240 (1955) 2333.